frontiers | Frontiers in Earth Science

TYPE Original Research
PUBLISHED 08 December 2022
DOI 10.3389/feart.2022.1041453

OPEN ACCESS

EDITED BY
Numair Siddiqui,
University of Technology Petronas, Malaysia

REVIEWED BY
Agus Ramdhan,
Institut Teknologi Bandung, Indonesia
Aqsa Anees,
Yunnan University, China

*CORRESPONDENCE
Tamer Abu-Alam,
tamer.abu-alam@uit.no
Mohamed Abioui,
m.abioui@uiz.ac.ma

SPECIALTY SECTION
This article was submitted to Solid Earth Geophysics, a section of the journal Frontiers in Earth Science

RECEIVED 10 September 2022
ACCEPTED 25 November 2022
PUBLISHED 08 December 2022

CITATION
Farouk S, Sen S, Abu-Alam T, Al Kahtany K and Abioui M (2022), Geomechanical assessment of the Lower Turonian AR-F limestone Member, Abu Gharadig Field, Egypt: Implications for unconventional resource development.
Front. Earth Sci. 10:1041453.
doi: 10.3389/feart.2022.1041453

Geomechanical assessment of the Lower Turonian AR-F limestone Member, Abu Gharadig Field, Egypt: Implications for unconventional resource development

Sherif Farouk[1], Souvik Sen[2], Tamer Abu-Alam[3]*, Khaled Al Kahtany[4] and Mohamed Abioui[5,6]*

[1]Exploration Department, Egyptian Petroleum Research Institute (EPRI), Cairo, Egypt, [2]Geologix Limited, Mumbai, Maharashtra, India, [3]The Faculty of Biosciences, Fisheries and Economics, UiT The Arctic University of Norway, Tromsø, Norway, [4]Department of Geology and Geophysics, College of Science, King Saud University, Riyadh, Saudi Arabia, [5]Department of Earth Sciences, Faculty of Sciences, Ibn Zohr University, Agadir, Morocco, [6]MARE-Marine and Environmental Sciences Centre—Sedimentary Geology Group, Department of Earth Sciences, Faculty of Sciences and Technology, University of Coimbra, Coimbra, Portugal

This study evaluates the unconventional reservoir geomechanical characteristics of the Lower Turonian Abu Roash-F (AR-F) carbonates from the Abu Gharadig field, onshore Egypt, which has not been attempted before. The interval dominantly consists of planktic foraminifera and micrite matrix. The AR-F marine carbonate is organic-rich (0.59–3.57 wt% total organic carbon), thermally mature (435–441°C T_{max}) and falls within the oil generation window. The studied interval is very tight with up to 2.6% porosity and 0.0016–0.0033 mD permeability with the wireline log-based brittleness index ranging between 0.39–0.72 which indicates a less brittle to brittle nature. AR-F exhibits a hydrostatic pore pressure gradient with minimum horizontal stress (S_{hmin}) varying between 0.66–0.76 PSI/ft. Safe wellbore trajectory analysis was performed for deviated and horizontal wells to infer the mud pressure gradients required to avoid wellbore instabilities. Based on the inferred in-stress magnitudes and considering an NNE regional maximum horizontal stress orientation, none of the fractures are found to be critically stressed at present day. To produce from the AR-F, hydraulic fracturing is necessary, and we infer a minimum pore pressure increment threshold of 1390 PSI by fluid injection to reactivate the vertical fractures parallel to regional minimum horizontal stress azimuth.

KEYWORDS

geomechanics, unconventional reservoir, AR-F carbonate, Abu Gharadig, Egypt

Introduction

Unconventional self-sourced reservoirs are well documented from the Northern American basins which revolutionized the shale gas and shale oil resource exploitation. Many of those resources are carbonate-dominated, e.g., Eagle Ford (Ozkan et al., 2013). Similar resources have also been reported from the Ordovician carbonates of the Ordos and Tarim basins of China (Wei et al., 2017; Chen et al., 2020). Recent studies have also focused on such potential tight carbonates from various parts of the world including offshore Malaysia (Bashir et al., 2021), Pakistan (Ali et al., 2022; Ullah et al., 2022), and China (Jiang et al., 2022). Three recent works by Boutaleb et al. (2021), Radwan et al. (2021) and Fea et al. (2022) reported self-sourcing and self-storing unconventional carbonate intervals from the African continent. Boutaleb et al. (2021) characterized the potential of Turonian anoxic carbonates from the Constantine Basin of northern Algeria, while Radwan et al. (2021) reported similar reservoir characteristics from the Eocene Radwany Formation of Gulf of Suez, Egypt; finally, Fea et al. (2022) study the reservoir quality discrimination of the Albian-Cenomanian reservoir sequences in the Ivorian Basin. The three reservoirs are organic-rich, tight and exhibit similar petrophysical signatures.

The northern Africa experienced a major eustatic sea-level rise during the Turonian-Cenomanian, which led to an anoxic deep marine condition (e.g., Herbin et al., 1986; Klemme and Ulmishek, 1991; Luning et al., 2004, and references therein). During this period, organic-rich carbonate sediments were deposited (Zobaa et al., 2009). One such example is the Lower Turonian Abu Roash-F Member (AR-F) of the Abu Gharadig field, onshore Egypt (Zobaa et al., 2011), which has been the primary focus of this study. The clastic and carbonate intervals from the Cenomanian Bahariya Formation, Upper Turonian AR-C and AR-E members are the primary hydrocarbon-producing reservoirs of the Abu Gharadig field (Hewaidy et al., 2018). AR-F is the proven source rock of the Abu Gharadig Basin (AGB) (Ghassal et al., 2018). Researchers have studied the AR-F from various parts of the Western Desert, Egypt (e.g., Bayoumi and Lotfy, 1989; Abdel-Kireem et al., 1996; Hantar, 1990; El-Sherbiny, 2002; El Beialy et al., 2010; El Atfy, 2011; Zobaa et al., 2011; El Diasty, 2014; Makky et al., 2014; Adly et al., 2016; Ghassal et al., 2018; Sarhan and Basal, 2020; Yang, 2020; Farouk et al., 2022, and others) and characterized its depositional environment, organic geochemical properties and source rock potential. However, its potential as an unconventional reservoir and its geomechanical properties had neither been addressed nor attempted. We took this opportunity to address the knowledge gap regarding the AR-F member.

Geomechanical characterization of the unconventional AR-F interval has been the primary objective of this study, which is the first of a kind from the onshore Western Desert, Egypt. Based on the results, suitable reservoir development strategies are briefly discussed for the unconventional AR-F carbonate interval. This work is timely and important, given the fact that the operators in the Western Desert are looking beyond the long-producing proven conventional reservoirs (AR-G Member, Bahariya Formation, *etc.*) to increase the resource base. Recently, the tight carbonates of the Upper Turonian AR-D Member have been successfully stimulated and put into production, which was otherwise excluded from the completion (for not being the primary reservoir target). These approaches are critically important to increase the domestic hydrocarbon production from existing fields using the readily available surface facilities and infrastructures which provides the opportunity for early monetization with a tremendous positive impact on project economics and the country's energy output.

In this work, we have integrated the available petrographic thin sections, petrophysical measurements from routine core analysis, organic geochemical data from rock-eval pyrolysis and wireline logs. We briefly characterized the unconventional reservoir characteristics of the studied AR-F Member. Under geomechanical analysis, we presented the log-based rock strength, dynamic elastic properties, brittleness index, pore pressure, and *in situ* stress magnitudes. Based on these rock-mechanical assessments and regional geological understanding, we discussed the unconventional reservoir development aspects which involve horizontal well placement, optimum mud weight requirement to achieve wellbore stability, and fracture reactivation potential because of fluid injection-induced shear slippage. Future scope and recommendations have been provided which will help the subsurface community to better plan the AR-F resource exploitation.

Geological settings

The Abu Gharadig Basin (AGB) is an E-W trending intra-cratonic rift basin located in the northern part of the Western Desert, Egypt (Figure 1). The basin is separated from the northern rift basins by the Qattara Ridge and Sharib-Sheiba Ridge. Its southern extent is bounded by the Kattaniya Ridge (Guiraud and Maurin, 1992; Shalaby and Sarhan, 2021). Rifting phase prevailed during the Jurassic to Early Cretaceous and ceased during the Late Cretaceous. Post-rifting phase is marked by a NW compression of the Alpine orogeny, which continued from the Late Cretaceous to the Tertiary period (Salama et al., 2021). Bosworth et al. (2008) inferred that the northern AGB was majorly affected by a compressional shortening. Subsequently, this formed NE-SW trending compressional structures and NW-SE to ESE-WNW trending extensional structures that culminated with a period of uplift, followed by erosion during the Santonian (Sarhan, 2017). Several structural traps were created during the basin inversion process (Sarhan and Collier, 2018). The study area, the Abu Gharadig field is one of the most prolific

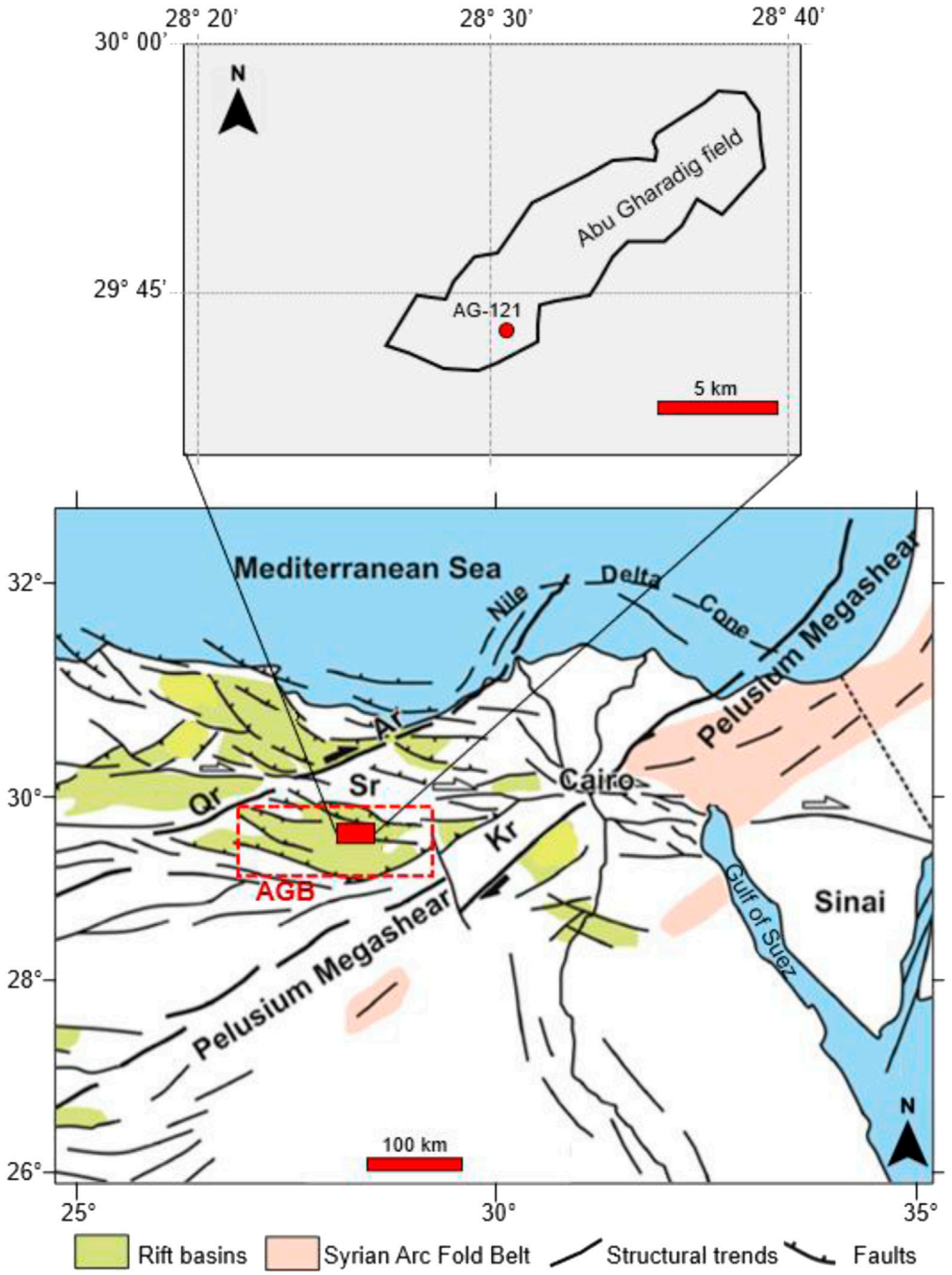

FIGURE 1
Location Map of the study area within Abu Gharadig Basin (AGB) in the Western Desert along with the major structural features (Qr, Qattara Ridge; Sr, Sharib-Sheiba Ridge; Kr, Kattaniya Ridge). Adapted from Shalaby and Sarhan (2021).

hydrocarbon discoveries from the AGB (El Gazzar et al., 2016). The study area is situated in the central AGB, between latitudes 29.35°–30°N and longitudes 28.2°–28.5°E. The field hosts roughly 12,000 feet of mixed siliciclastic and carbonate sediments of the Cretaceous to Paleogene age. During the Late Cretaceous post-rift stage, major transgressive cycles and inundation deposited carbonate-dominated successions while minor clastic sedimentation occurred during the shorter regressive cycles. During the Late Cretaceous transgressive event, Abu Roash and

Bahariya formations were deposited in fluvio-marginal marine to shallow marine environment (Sarhan, 2017). The Abu Roash (AR) Formation conformably lies above the Bahariya Formation and is subdivided into seven distinct members, marked as A-G. Moretti et al. (2010) discussed the petroleum system elements of the Western Desert and identified mature source rock intervals in the Cretaceous Alam El Bueib and Abu Roash Formations and identified thermally immature source rocks in the Cenozoic Apollonia Formation. Researchers have interpreted that the AR-F limestones are the main source rock of the AGB (Adly et al., 2016; Ghassal et al., 2018). Hydrocarbons are primarily trapped in the crest of the Mesozoic tilted blocks with hydrocarbon migration being influenced by fault hydraulic behavior (Strating and Franssen, 2006; Moretti et al., 2010). AR-C and AR-E host the primary clastic reservoirs deposited during the Upper Turonian, while the Cenomanian reservoir is hosted by the Bahariya sandstones. Late Cretaceous shales are inferred as the main seal or cap rocks laying above the Abu Roash and Bahariya reservoirs (e.g., El Shahat et al., 2009; Moretti et al., 2010; Kassem et al., 2021a, b; Kassem et al., 2022). Our study focuses on the AR-F Member which is composed of carbonates.

Materials and methods

We studied a recently drilled vertical well where 110 feet of core was recovered from the AR-F Member between 10,370 ft and 10480 ft. We analyzed petrographic thin sections, scanning electron microscopy (SEM), core-measured porosity and horizontal permeability, total organic carbon (TOC) measured by the Leco C230 system, and T_{max} determined by Rock-Eval 6 Pyrolizer to characterize the studied AR-F interval. Wireline logs have been the primary input for geomechanical assessment. Rock elastic properties, i.e., Poisson's ratio (υ) and Young's modulus (E) from sonic velocity and density logs:

$$\upsilon = \frac{Vp^2 - 2Vs^2}{2(Vp^2 - Vs^2)} \tag{1}$$

$$E = \rho b * Vs^2 \left[\frac{3Vp^2 - 4Vs^2}{Vp^2 - Vs^2}\right] \tag{2}$$

where, Vp and Vs are compressional and shear sonic velocities, respectively, ρb denotes the formation bulk density. We followed Militzer and Stoll (1973) to estimate unconfined compressive strength (UCS) using question 3:

$$UCS = \frac{\left(\frac{7682}{DTC}\right)^{1.82}}{145} \tag{3}$$

where DTC is compressional sonic slowness. The coefficient of internal friction (μ) was estimated by Lang et al. (2011):

$$\mu = \tan\varphi = \tan\left[Sin^{-1}\left(\frac{Vp - 1}{Vp + 1}\right)\right] \tag{4}$$

where Vp is the compressional sonic velocity in km/second, φ is friction angle in degrees. Based on the log-based dynamic elastic properties, we have estimated the brittleness index (BI) of the AR-F Member following Grieser and Bray's (2007) model utilizing Eq. 5:

$$BI = \frac{1}{2}\left[\frac{E - Emin}{Emax - Emin} + \frac{\upsilon - \upsilon\,min}{\upsilon\,max - \upsilon\,min}\right] \tag{5}$$

Since AR-F is not a producing/proven primary reservoir, therefore direct downhole pressure measurements were not recorded. We utilized drilling mud pressure as a pore pressure proxy against the AR-F interval. Vertical stress (S_v) was estimated from the bulk-density log (Plumb et al., 1991):

$$S_v = \int_0^H \rho b(H) * g\, dH \tag{6}$$

where H denotes true vertical depth. Since the targeted AR-F interval is carbonate, a normal compaction trend line-based pore pressure estimation approach could not be utilized. Therefore, formation pore pressure (PP) was inferred based on the drilling mud weight being used as a PP proxy. Well-completion reports and daily drilling reports were studied to decipher any well events that might have occurred during drilling (formation fluid influx *etc.*) which can provide additional information about the downhole mud overbalance characteristics (difference between drilling mud pressure and PP). For minimum horizontal stress (S_{hmin}), we followed Poisson's ratio-based Eaton's uniaxial model (Eaton, 1968):

$$S_{hmin} = \frac{\upsilon}{1 - \upsilon}(S_v - PP) + PP \tag{7}$$

Maximum horizontal stress (S_{hmax}) is a difficult parameter to calculate, especially in absence of image log-based breakout widths. We followed a simplistic approach by Lang et al. (2011), defined as:

$$S_{hmax} = S_{hmin} + k\,(S_v - S_{hmin}) \tag{8}$$

where "k" is an effective maximum horizontal stress ratio factor. Its value ranges between 0–2 (Lang et al., 2011). S_{hmax} can be calibrated with image log-based breakout widths which will provide a confident estimate of "*k*." However, the image log had not been recorded against AR-F interval in any of the wells since this was not a primary reservoir of the Abu Gharadig field. Zhang (2013) suggested $k < 1$ for normal faulting regimes and $k \geq 1$ for other stress states. In general, Abu Gharadig Basin is an intra-cratonic rift basin and we have considered $k = 0.5$. However, recent studies have reported present-day normal faulting to strike-slip transitional stress state from the onshore Nile Delta (Leila et al., 2021). Based on the inferred geomechanical parameters, we employed Mohr-Coulomb

failure criteria to decipher the shear failure gradient (SF) which denotes the minimum required mud weight for avoiding compressive failures (Zhang, 2013; Zhang et al., 2015):

$$SF = \frac{\{3S_{hmax} - S_{hmin} - UCS + (Q-1)*PP\}}{Q+1} \quad (9)$$

$$\text{Where, } Q = \frac{(1+Sin\,\mu)}{(1-Sin\,\mu)} \quad (10)$$

In deviated wells, *in situ* stresses should be transformed into a new Cartesian coordinate system (x, y, z) associated with well orientation. For a well with inclination "*i*" drilled in a direction of "θ" with respect to the regional S_{hmax} azimuth, the *in situ* stresses in (x, y, z) space are defined as (Abbas et al., 2019):

$$\sigma_x = (S_{hmax}\,Cos^2\theta + S_{hmin}\,Sin^2\theta)\,Cos^2 i + S_V Sin^2 i \quad (11)$$

$$\sigma_y = S_{hmax}Sin^2\theta + S_{hmin}Cos^2\theta \quad (12)$$

$$\sigma_{zz} = (S_{hmax}Cos^2\theta + S_{hmin}Sin^2\theta)Sin^2 i + S_v Cos^2 i \quad (13)$$

$$\tau_{xy} = 0.5\,(S_{hmin} - S_{hmax})\,Sin\,2\theta Cosi \quad (14)$$

$$\tau_{xz} = 0.5\,(S_{hmax}Cos^2\theta + S_{hmin}Sin^2\theta - S_v)\,Sin\,2i \quad (15)$$

$$\tau_{yz} = 0.5\,(S_{hmin} - S_{hmax})\,Sin\,2\theta Sini \quad (16)$$

In a cylindrical system (r, z, θ) the stress components are presented as radial stress (σ_r), tangential stress (σ_θ) and axial stress (σ_z). These are resolved by Kirsch's equations. At the borehole wall, these are transformed as (Abbas et al., 2019):

$$\sigma_r = MP \quad (17)$$

$$\sigma_\theta = (\sigma_x + \sigma_y) - 2(\sigma_x - \sigma_y)\,Cos\,2\theta - 4\tau_{xy}\,Sin\,2\theta - MP \quad (18)$$

$$\sigma_z = \sigma_{zz} - 2\theta\,(\sigma_x - \sigma_y)\,Cos\,2\theta - 4\theta\tau_{xy}\,Sin\,2\theta \quad (19)$$

$$\tau_{\theta z} = 2\,(-\tau_{xz}\,Sin\,\theta - \tau_{yz}\,Cos\,\theta) \quad (20)$$

where MP is the drilling mud pressure. Considering zero shear stresses, the effective principal stresses, therefore, can be written as (Abbas et al., 2019):

$$\sigma_{tmax} = 0.5\left(\sigma_z + \sigma_\theta + \sqrt{(\sigma_z - \sigma_\theta)^2 + 4\,(\tau_{\theta z})^2}\right) \quad (21)$$

$$\sigma_{tmin} = 0.5\left(\sigma_z + \sigma_\theta - \sqrt{(\sigma_z - \sigma_\theta)^2 + 4\,(\tau_{\theta z})^2}\right) \quad (22)$$

where σ_{tmax} and σ_{tmin} denote the highest and the least stresses respectively, which are dependent on the well trajectory in the case of deviated wells. Based on the well trajectory (inclination and azimuth) and resolved stresses, SF is calculated along the well path for safe wellbore trajectory analysis and recommendations are provided regarding the deviated/horizontal well placement to ensure the geomechanical integrity of the wellbores. Based on the estimated *in situ* stress magnitudes, we have inferred the slip/reactivation potential of weak planes (i.e., fractures, *etc.*). These planes can experience shear slippage if the shear stress acting on the fracture planes exceeds the shear strength during fluid injection (e.g., Zoback and Lund Snee, 2018). Following Coulomb failure criteria, the critical pore pressure (CPP) limit to cause slippage on a randomly oriented fracture plane is estimated as (Taghipour et al., 2019):

$$CPP = \frac{1}{2}\,(3S_3 - S_1) \quad (23)$$

where S_3 and S_1 are the minimum and maximum principal stresses. In a normal faulting stress regime, $S_3 = S_{hmin}$ and $S_1 = S_v$. Eq. 23 assumes no change in total stresses and negligible cohesion on the fracture planes, thus providing a very conservative estimate.

Results

Characteristics of AR-F member

The thin section analysis indicates the dominance of the micrite matrix (31%–50.5%) in all samples (Figure 2). Planktic foraminifera is the principal skeletal grain (~35%) observed along with calcispheres, pelecypods, pelagic bivalves, echinoderms, and pyrites. The visual porosity is negligible. Thin sections reveal fracture porosity due to the shattering of grains with very poor pore interconnectivity. The muddy allochem limestones of AR-F typically represent pelagic deep water basinal facies. The dominance of the planktic forams and absence of the benthic forams indicate calm conditions and low-energy waves (Flügel, 2010). Accordingly, an open marine basinal depositional environment (between 100 m and 300 m) can be assigned to the studied interval (Flügel, 2010). The measured TOC values of the analyzed AR-F samples vary between 0.59 and 3.57 wt% (Figure 2) with an average TOC value of 2.2 wt%. Most of the data suggest TOC >1.5 wt%. We followed the TOC classification proposed by Peters (1986), which has been extensively utilized by researchers, for source rock characterization (Kenomore et al., 2017; Kumar et al., 2017; Hakimi et al., 2018; Harishidayat et al., 2022). Based on this classification, the AR-F Member has fair to very good organic richness. Ghassal et al. (2018) also reported a similar TOC range (0.32%–4.37%) from the GPT field, southern AGB, while Makky et al. (2014) reports 1.27–4.46 wt% TOC from the AR-F of West Beni Suef concession, Western Desert. The pyrolysis T_{max} values range from 435–441°C and have an average value of 438.5°C (Figure 2), which signifies that the AR-F is thermally mature and falls within the oil generation window. These measured values correlate well with the observations made by previous researchers (Makky et al., 2014; Ghassal et al., 2018) which provided a T_{max} range of 421–430°C against AR-F carbonates from other parts of the Western Desert. The routine core analysis indicates that the AR-F Member is very tight with 0.9%–2.6% porosity and 0.0016–0.0033 mD horizontal permeability (Figure 2). The SEM images also reveal isolated nanopores confirming the tight behavior. The gas chromatograph data from mud logging of the studied well indicated around 2,000 ppm of methane (C_1) and 300 ppm of

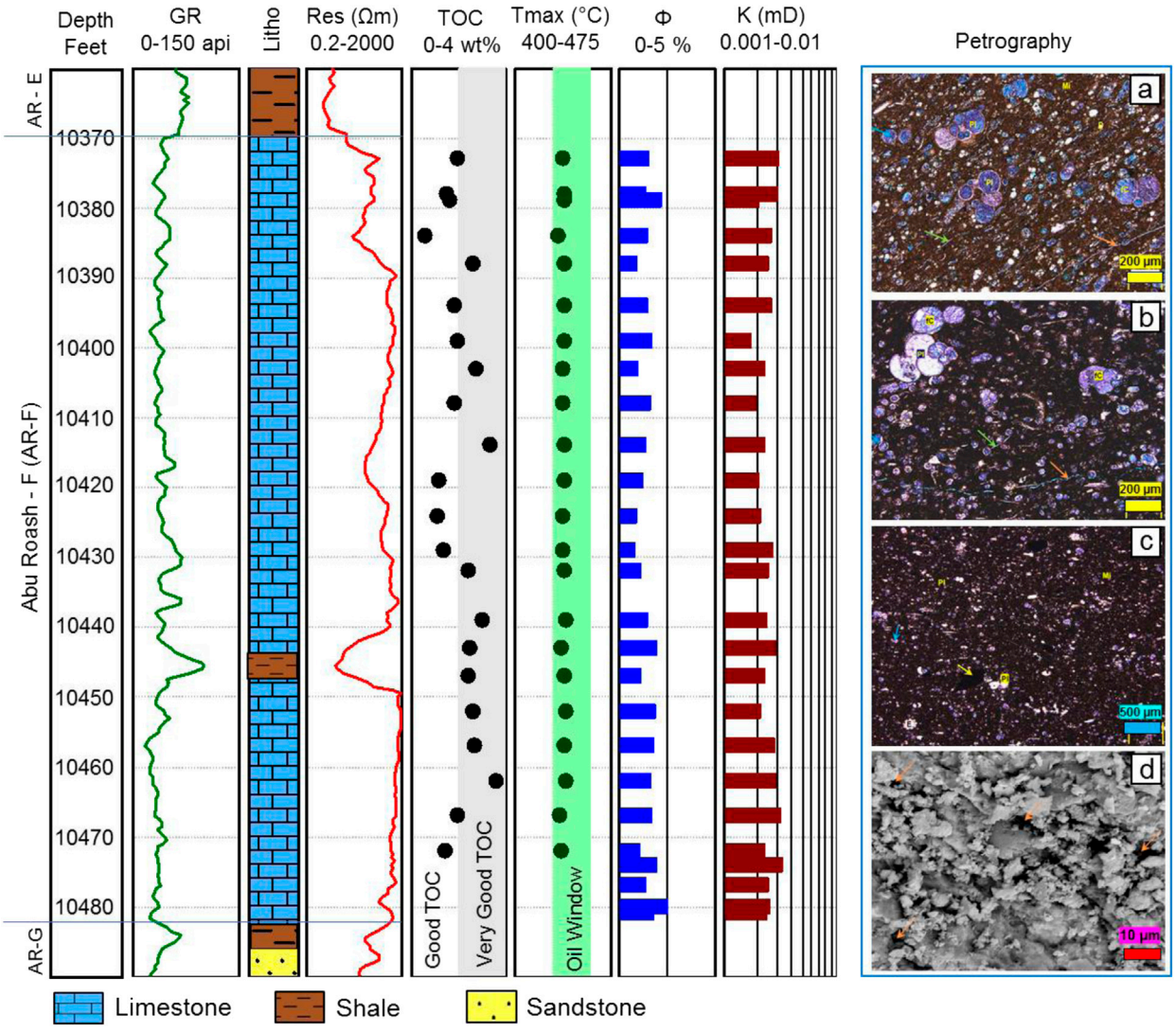

FIGURE 2
Geochemical (TOC and T_{max} from Rock-Eval pyrolysis), petrophysical properties (Φ and K from routine core analysis), petrographic thin sections and SEM image of the studied AR-F interval. Thin sections **(A–C)** indicate the presence of micrite matrix along with frequent planktic foraminifera, minor pelagic bivalves (green arrow), black pyrite crystals (yellow arrows), and thin fractures (orange arrows); **(D)** SEM indicates isolated nanopores.

ethane (C_2) in the upper part of the AR-F between 10,370 and 10420 feet. The lower part of the AR-F (10,430–10470 feet) is associated with much higher C_1 (10,000–40000 ppm) and C_2 concentrations (1,000–4,000 ppm). This lower interval with higher gas content coincides with the high TOC (>2.5 wt%) interval of the AR-F.

Rock-mechanical properties and brittleness index

Wireline log-based dynamic rock-mechanical assessment indicates an average υ of 0.29, E ranging between 23 and 47 GPa, and an average μ of 0.7 (Figure 3). Sonic slowness-based UCS varies between 33 and 55 MPa.The υ and E-based brittleness analysis indicate a BI range of 0.39–0.72 (Figure 3). The upper interval of AR-F exhibits BI > 0.48, indicating a more brittle nature than the lower part, which exhibits 0.32 < BI < 0.48 (i.e., less brittle). Higher TOC content in the bottom part of AR-F (Figure 2)corroborates well with the lower BI observations. The estimated rock-mechanical properties and BI are plotted against core-measured organic content (TOC) in Figure 4. It exhibits an increase in υ with TOC (Figure 4B). Rock stiffness (E) and strength (UCS) decrease with more organic content (Figures 4A,C). The brittleness index decreases with TOC (Figure 4D), as higher organic content introduces ductility.

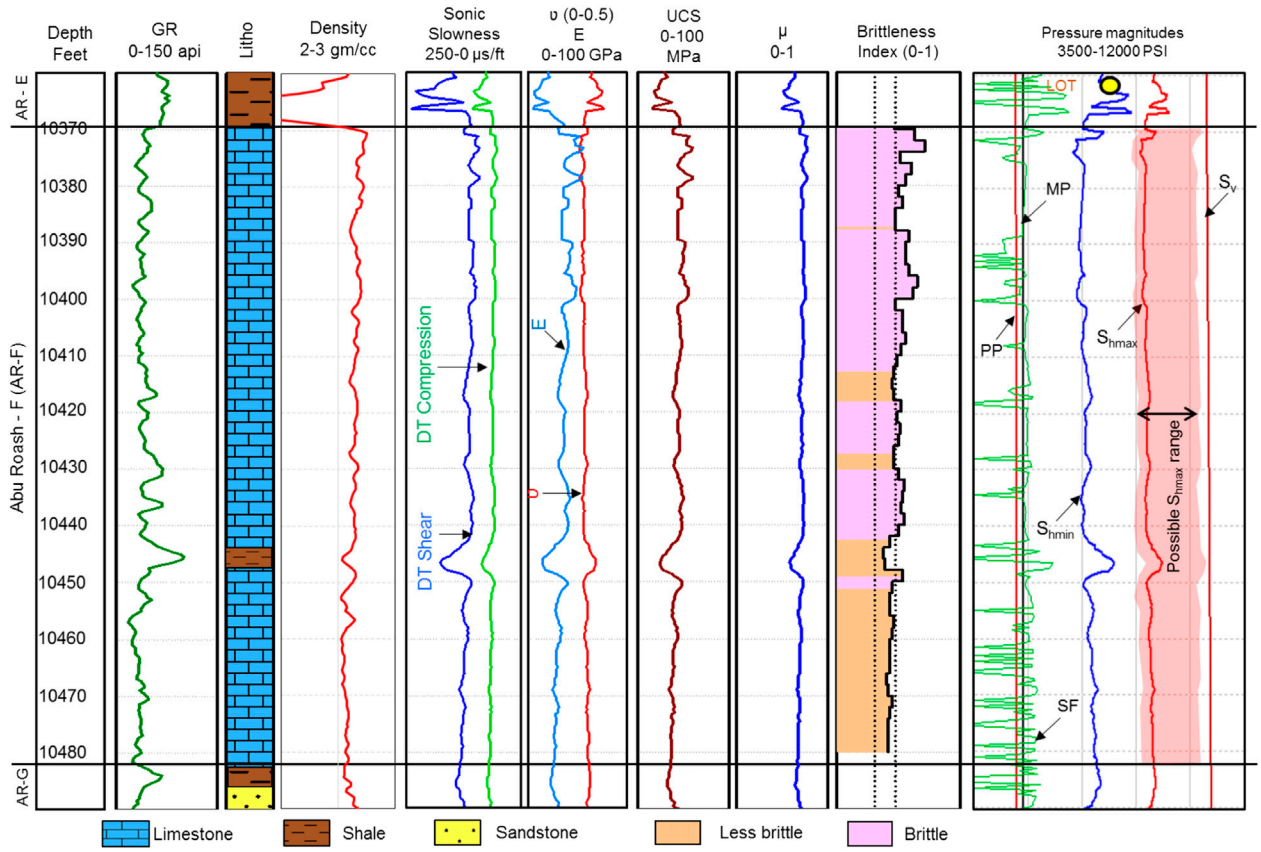

FIGURE 3
Well log-based rock-mechanical properties (E, υ, UCS, and µ), brittleness index, pore pressure (PP), shear failure pressure (SF) and *in situ* stress magnitudes (S_v, S_{hmin}, and S_{hmax}) of the studied AR-F interval. LOT, Leak-off test; PP, formation pore pressure; MP, drilling mud pressure.

Pore pressure and *in situ* stress distribution

Bulk-density-based S_v indicates an average gradient of 1.05 PSI/ft (Figure 3). In absence of direct pressure measurement, we utilized drilling fluid pressure as a PP proxy, considering downhole mud overbalance being maintained during drilling. The AR-F carbonate interval in the studied well was drilled with a mud pressure gradient of 0.50 PSI/ft (Figure 3). The well completion reports did not mention any connection gas or formation fluid influx event during drilling, which confirms that sufficient mud overbalance was maintained. The lowest mud weight gradient utilized to drill this section in the offset wells was observed as 0.48 PSI/ft. Therefore we can conclude that the PP gradient of AR-F in the studied field is definitely less than 0.48 PSI/ft. We inferred a hydrostatic pore pressure gradient of 0.45PSI/ft within AR-F. Considering the drilling mud weight (~0.47 PSI/ft) as the highest pore pressure threshold, there is a maximum uncertainty of ~190 PSI in PP magnitude.

The υ-based S_{hmin} yielded a gradient range of 0.66–0.76 PSI/ft within AR-F (Figure 3). We had one leak-off test record (7988 PSI at 10,362 ft) from the overlying shales of the AR-E Member which exhibited a S_{hmin} gradient of 0.77 PSI/ft. The interpreted AR-F S_{hmin} gradient corroborates well with the published interpretation from the JDT field and Al-Khilala fields located in the onshore Nile Delta region (Salah et al., 2016; Leila et al., 2021). Considering a normal faulting stress state and an effective maximum horizontal stress ratio (k) of 0.5, we infer a S_{hmax} gradient of 0.88 PSI/ft. It is to be noted that the estimated S_{hmax} could not be calibrated due to the unavailability of the image logs. However, Leila et al. (2021) reported a 0.86–1 PSI/ft S_{hmax} range from the onshore Al Khilala field depicting a normal to strike-slip transitional stress regime in the Nile Delta. Following this inference of normal faulting stress state, we have provided the regional S_{hmax} range in Figure 7, while our calculated S_{hmax} estimate can be considered as a lower estimate.

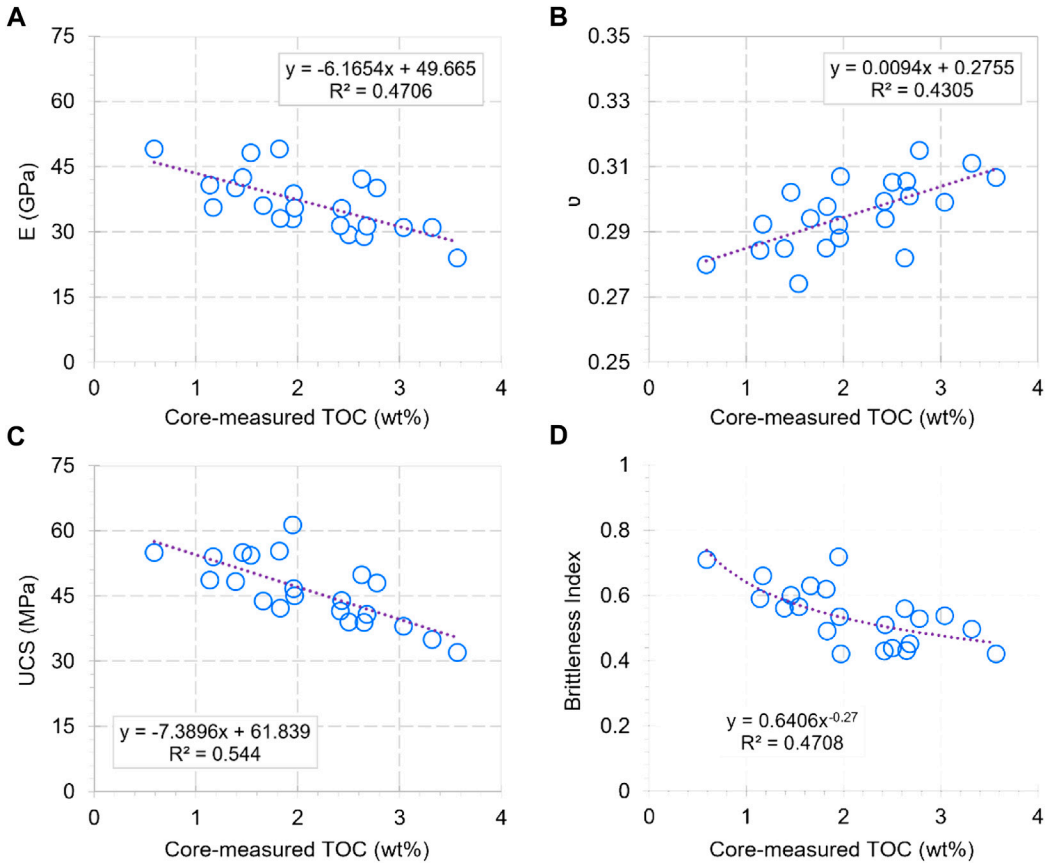

FIGURE 4
Relationship of core-measured TOC with **(A)** Young's modulus, **(B)** Poisson's ratio, **(C)** UCS and **(D)** brittleness index.

Discussions

Diagenetic effects on reservoir properties

Petrophysically, the AR-F exhibits very poor storage and flow capacity. Micritization, the dominant diagenetic process, has been identified as a reservoir quality-destroying factor. This occurs during the first diagenetic phase and usually fills up the pore throats and reduces the permeability. Bioclast tests and chambers are found to be filled with calcite cement which also contributed to the cementation-related porosity loss. We identified frequent thin fractures in the petrographic analysis, which indicate the presence of minor mechanical compaction. These fractures may locally improve the reservoir quality. However, these fractures are mostly seen to be filled with calcite cement, which, therefore, did not improve the flow capacity of AR-F. To bring this tight unconventional carbonate reservoir into production, stimulation is certainly required.

Horizontal well placement and borehole stability

Horizontal well drilling through the AR-F with a slotted liner completion strategy is an effective way to ensure maximum reservoir contact (Salamy et al., 2008), as these perforated liners also provide increased accessibility for coil tubing (CT) as well as acid jobs. The studied vertical well indicates around 0.52 PSI/ft shear failure gradient (SF) against the AR-F carbonate interval (Figure 3), which is very close to the drilling mud pressure. Therefore, any severe wellbore instability was not observed. However, the SF value will vary in a deviated/horizontal well based on the well inclination and its azimuth with respect to the regional S_{hmax} orientation. World Stress Map (WSM) database indicates an N-S to NNE-SSW S_{hmax} azimuth. A horizontal well drilled parallel to E-W direction will be the most suitable choice for such tight carbonate reservoir development since this will facilitate geomechanically optimum hydraulic fracture propagation parallel to N-S, thus creating a transverse

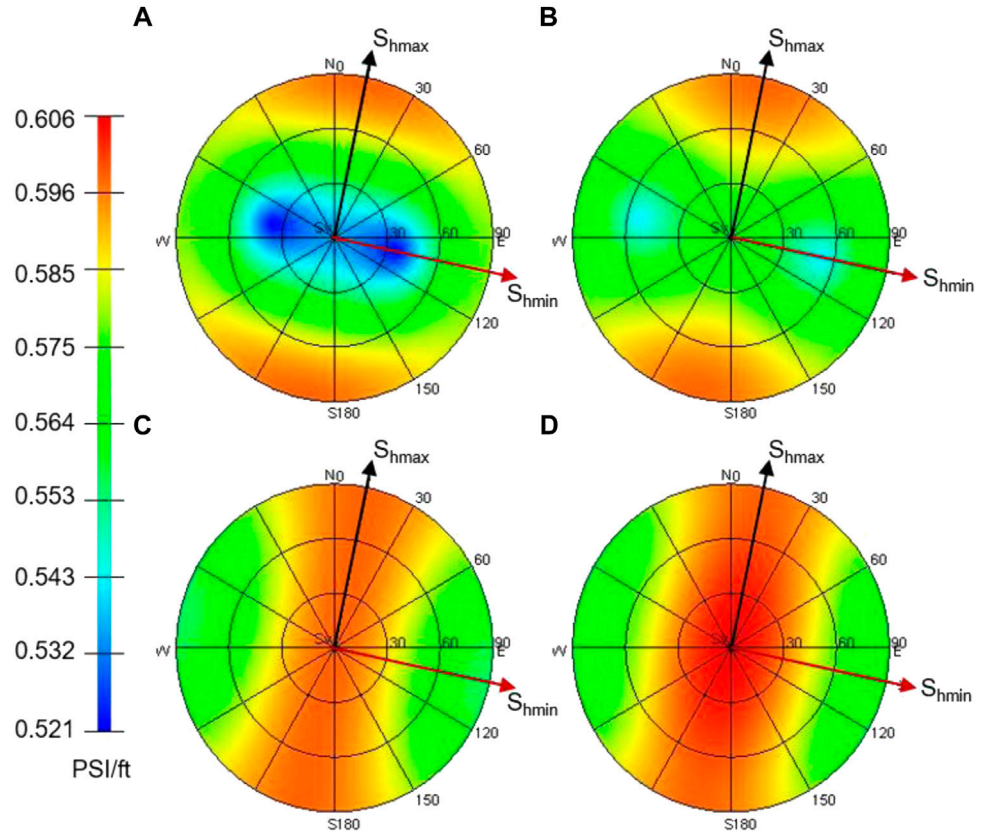

FIGURE 5
Safe wellbore trajectory analysis and minimum mud pressure requirements (refer to the colour bar for mud pressure gradient scale) to avoid compressive wellbore failure, **(A)** $S_{hmax} << S_v$, **(B)** $S_{hmax} < S_v$, **(C)** $S_{hmax} = S_v$ and **(D)** $S_{hmax} > S_v$. In this mud pressure circular plot (lower hemisphere plot) well azimuth is plotted along the periphery of the circle and well inclination is plotted along the radius. Centre of each circle denotes the vertical well position, and a horizontal well at any azimuth will be plotted on the periphery.

fracture network. Leila et al. (2021) reported an NNE (12°N) regional S_{hmax} orientation from wellbore failures in the onshore Nile Delta region. Considering the same horizontal stress azimuth, we inferred the minimum mud weight requirements in a deviated or horizontal well to avoid shear failure and ensure wellbore integrity. Results are presented in Figure 5 which indicates a higher mud weight requirement in deviated wells for wellbore stability when compared to a vertical well. Since the estimated S_{hmax} could not be calibrated, therefore the S_{hmax} magnitude contains uncertainties. To reduce the uncertainties in inferring the wellbore stability, we simulated the mud weight requirements at various S_{hmax} gradient scenarios. S_v gradient has been used as 1.05 PSI/ft, while for S_{hmin} we utilized the lower gradient estimate of 0.66 PSI/ft. Figure 5A depicts a normal faulting scenario with a S_{hmax} gradient of 0.86 PSI/ft, which is the lowest value reported from the onshore Nile Delta by Leila et al. (2021). This normal faulting stress state exhibits a lower mud weight requirement of <0.543 PSI/ft for deviated wells up to 45° well inclination along the S_{hmin} azimuth, while a horizontal well along S_{hmin} azimuth will require 0.57 PSI/ft mud gradient. A slight increase in the S_{hmax} gradient to 0.88 PSI/ft exhibits lower mud pressure requirements for 40–60° well inclination along the S_{hmin} azimuth (Figure 5B), while deviated wells parallel to S_{hmax} orientation will require a much higher mud weight (~0.59 PSI/ft) to maintain wellbore stability (Figure 5B). Figure 5C considers $S_{hmax} = S_v = 1.05$ PSI/ft, which indicates a higher mud pressure requirement (>0.58 PSI/ft) in vertical/deviated/horizontal wells if drilled parallel to S_{hmax} azimuth (12°N), the same is also applicable for deviated wells up to 30° inclination when drilled along S_{hmin} azimuth. In a strike-slip stress state ($S_{hmax} > S_v =$ 1.05 PSI/ft), vertical wells and any deviated well drilled parallel to S_{hmax} are observed to be the least stable and will therefore require a higher mud pressure (>0.59 PSI/ft). Considering the results from all stress states (Figures 5A–D), we infer that the wells with >40° inclination along S_{hmin} will be the most stable well profiles in terms of wellbore stability, irrespective of stress states and S_{hmax} magnitudes. Since maximum reservoir contact will be a primary necessity and thus horizontal wells, drilling the same along S_{hmin} will also ensure effective hydraulic fracture propagation parallel to the S_{hmax} azimuth. The overall brittle

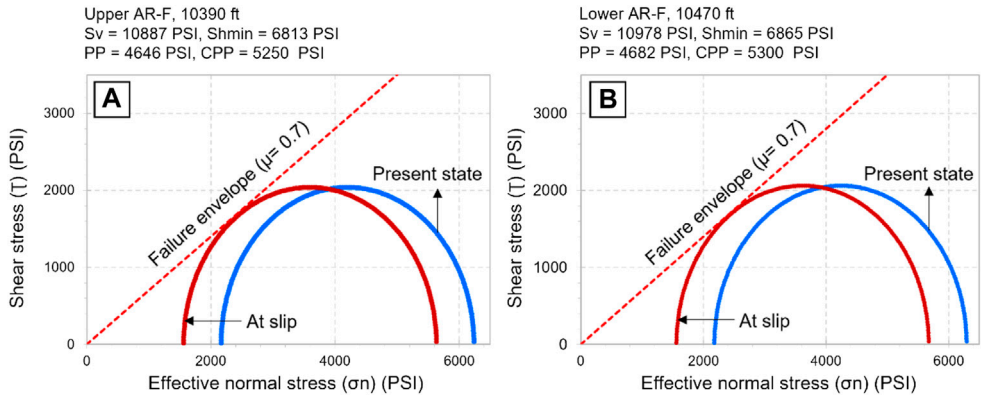

FIGURE 6
Criteria for shear slippage on a randomly oriented weak plane at **(A)** Upper AR-F and **(B)** Lower AR-F intervals. CPP denotes critical pore pressure for a slip to happen.

behavior of the AR-F indicates higher hydraulic fracturing success.

Fracture reactivation

We analyzed the effect of fluid injection-induced repressurization effect on the shear slippage of randomly oriented preexisting weak planes, i.e., faults, fractures, *etc*. To infer the failure limit, a linear Mohr failure envelope has been utilized considering aμ value of 0.7, as observed from the estimated rock-mechanical properties. With an increase in PP (due to fluid injection), the Mohr circle shifts to the left and eventually touches the failure envelope which marks the onset of failure (Figure 6). At upper and lower AR-F levels, approximately 5,250–5300 PSI of critical pore pressure can induce slippage (Figure 6). It is to be noted that this estimation provides a lower limit of downhole pressure build-up by injection since it considers zero cohesive strength of the formations, therefore the actual capacity for the formation to withstand the pressure buildup before failing will be much higher. Due to the fluid injection in the hydraulic fracturing (HF) process, the tendency of existing closed natural fractures to be activated by fluid injection is dependent on their orientations relative to S_{hmax} azimuth (Zoback and Lund Snee, 2018). The critically stressed fractures are more likely to get reactivated and participate in the flow network. Further increment in PP is capable of reactivating other fracture orientations, thus yielding a reactivated fracture network that enhances the success of hydraulic fracturing. Assuming the fractures to be vertical and based on our geomechanical estimates ($S_v > S_{hmax}$, μ=0.7) with a S_{hmax} azimuth of 12°N (Leila et al., 2021), we observe that none of the fractures are critically stressed at the present-day stress state. The fracture orientations between 70°N and 130°N (parallel to S_{hmin}) are the most stable ones while the fractures parallel to S_{hmax} could experience slip at an additional PP of 2,000 PSI (Figure 7A). Since we did not have any image log to calibrate the S_{hmax} magnitude, we also analyzed the fracture slip possibility in a normal to strike-slip transitional stress regime as depicted by Leila et al. (2021). Therefore, we assumed $S_v \approx S_{hmax}$ and performed the analysis (Figure 7B). The results indicate that the vertical fractures of 0°N–60°N azimuth are more sensitive to slip in such a stress state and may get reactivated with a much lesser PP increment by fluid injection, i.e., around 1390 PSI (Figure 7B). Since the absence of image log data makes the S_{hmax} calibration difficult, this result can be considered as a minimum PP increment threshold to achieve a fracture reactivation network that can successfully enhance the AR-F permeability by stimulation.

Future scope and recommendations

This study is based on a recently drilled vertical well where wireline logs, petrographic and petrophysical measurements were available from the studied AR-F Member. Since this is not the primary producer (i.e., zone of interest in terms of conventional reservoir pool), usually sonic logs were not recorded in the majority of the wells. Even in older wells, log data is unavailable for this interval, although organic geochemical characterization had been done on the AR-F cores and cutting samples from a few older wells (e.g., Abdel-Fattah et al., 2022; Khalil Khan et al., 2022). Availability of logs as well as laboratory-measured rock strength, and elastic properties are critical for any geomechanical analysis. Subsurface measurements and advanced logs like image logs provide useful insight into the formation behavior (i.e., compressive/tensile failures, bed boundaries, fracture orientations, *etc*.), and provide the opportunity to

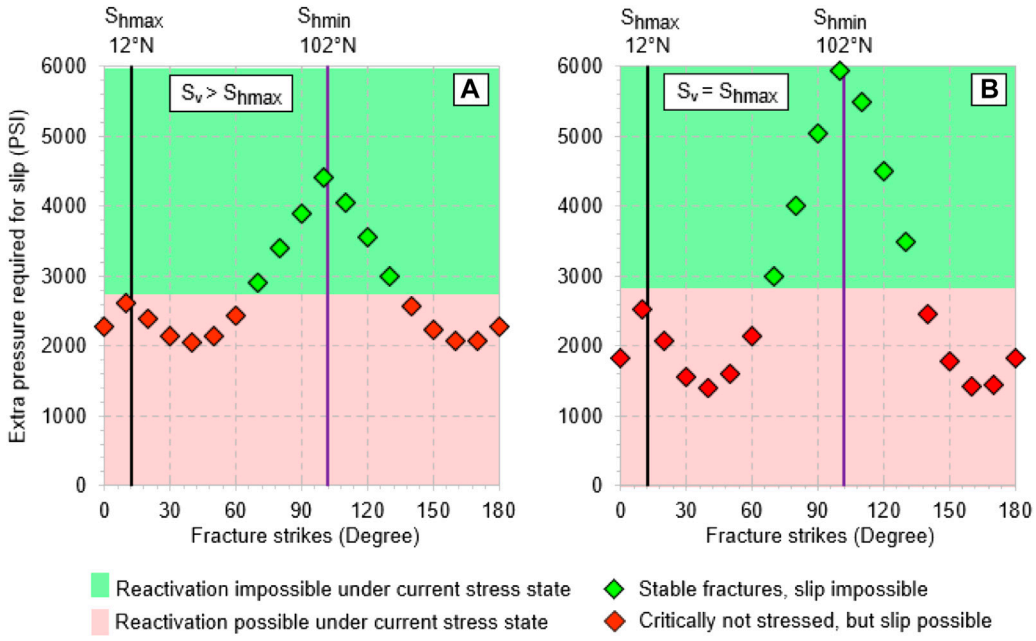

FIGURE 7
Natural fracture reactivation analysis after stimulation considering **(A)** normal stress regime and **(B)** normal to strike-slip transitional stress regime. The analysis assumes a maximum horizontal stress azimuth of 12°N (Leila et al., 2021), and a coefficient of internal friction (μ)=0.7.

calibrate geomechanical models (i.e., horizontal stress azimuth and S_{hmax} magnitude). These datasets and measurements were unavailable from the AR-F interval. Leak-off pressure measurement was recorded in the overlying shales of AR-E Member (Figure 3). LOT values overestimate S_{hmin} and actual S_{hmin} can be lesser than the estimated one. We recommend performing an extended leak-off test and gathering fracture closure pressure, which provides a better calibration for S_{hmin}. Cores should be taken out to perform triaxial tests which will provide direct calibration of UCS, cohesive strength and friction coefficient, which have presently been estimated from sonic logs. Core-based mineralogical analysis by X-ray diffraction (XRD) will provide mineralogy-derived brittleness estimates. Summarily, more data from future wells are required to extract further critical information on the AR-F characteristics in terms of geomechanical responses. This work presents preliminary findings and inferences based on single well data. In the future, with a greater number of wells covering the AR-F Member (logs, cores, and measurements, as discussed above), we can present a field-scale distribution of the geomechanical properties.

HF is a necessity to bring such tight intervals into production. There are ample examples of low porosity, low-permeability tight unconventional clastic and carbonate reservoirs worldwide which produces economically from horizontal wells stimulated by hydraulic fracturing (Curtis, 2002; Hajeri et al., 2007; Lin and Su, 2007; Hood and Yurewicz, 2008; Jarvie, 2012; Zhao et al., 2012; Lin et al., 2020). Recently a tight argillaceous limestone reservoir of AR-D Member of the Abu Gharadig field was tested for hydrocarbon potential. The tested interval exhibited similar tight nature to that of the studied AR-F and it did not flow naturally, but acid stimulation resulted in an economic flow rate (EGPC, 2019). A similar approach can be taken up for AR-F as well. Referring to the Middle Eastern tight carbonate reservoir development strategies (Salamy et al., 2008; Chimmalgi et al., 2013; Alyan et al., 2015; Sen et al., 2021) we recommend that coil tubing (CT) carried a gun and acid stimulation will be helpful to activate this tight reservoir. Saleri et al. (2004) discussed the utility of MRC (maximum reservoir contact) wells to achieve optimum reservoir performance and economic production rates from tight carbonate reservoirs in the Shaybah field of Saudi Arabia. Latief et al. (2019) discussed the utility of an underbalanced drilling strategy to enhance production from carbonate reservoirs with poor permeability. The authors reported a threefold oil production increase as the bottom hole pressure was reduced by 20% below formation pressure during underbalanced drilling with nitrogen injection (Latief et al., 2019). A similar strategy has yet not been tested in any Egyptian carbonate reservoir but is worth considering. Since the AR-F has not been tested yet to infer its production potential, we cannot comment on the economic viability of the studied interval. However, the initial assessment based on the integration of subsurface dataset exhibits promising results.

Conclusion

This is the first work focusing on the unconventional reservoir development aspects of the AR-F Member from the Abu Gharadig Basin. Based on the organic geochemical analyses and core-based petrophysical measurements, the studied deep marine AR-F carbonate interval is inferred as a self-sourced unconventional reservoir. Dynamic elastic properties indicate that the upper AR-F interval is more brittle than the lower part, which is also supported by the fact that lower AR-F is more organic-rich. Pore pressure and *in situ* stresses were estimated from well logs, drilling data, and direct measurements. We assessed the slip potential of vertical fractures exposed to hydraulic fracturing-induced pore pressure perturbations. At the present *in situ* stress state, we conclude that none of the fractures are critically stressed and therefore, we modeled the extra pore pressure build-up needed to reactivate the fractures parallel to the regional S_{hmin}, which are more prone to shear slippage. To validate its production potential, AR-F Member should be perforated and tested with the proposed strategies. If successful, it can be quickly brought into completion and production by combining it with already producing Abu Roash members and Bahariya intervals using the same infrastructures. The results of this study may help in further reservoir development.

Data availability statement

The original contributions presented in the study are included in the article/Supplementary Material, further inquiries can be directed to the corresponding authors.

Author contributions

SF supervised the project and was responsible for data management. SS conceptualized the idea, contributed to methodology, formal analysis, preparation of figures, and writing the original draft. All authors contributed to the literature review, data interpretation, reviewing, and revising of the original draft.

Funding

Open access funding is provided by UiT The Arctic University of Norway.

Acknowledgments

The authors thank Numair Siddiqui (Associate Editor) for the excellent editorial handling, and three reviewers for their constructive reviews. The authors are grateful to Egyptian General Petroleum Corporation (EGPC) for the dataset and permission to publish this study. SS acknowledges Geologix Limited or providing the GEO Suite of software that had been utilized in various analyses presented here. The authors thank Stanley T. Paxton (United States) for providing an internal review. Research Supporting Project number (RSP-2021/139), King Saud University, Riyadh, Saudi Arabia. This paper is a contribution to IGCP 679: Cretaceous Earth Dynamics and Climate in Asia. Finally, MA would like to dedicate this paper and express his best wishes to Full Abdelkrim Ezaidi (Ibn Zohr University, Morocco) for a happy retirement life filled with excellent health, excitement, and prosperity.

Conflict of interest

Author SS was employed by the company Geologix Limited.

The remaining authors declare that the research was conducted in the absence of any commercial or financial relationships that could be construed as a potential conflict of interest.

Publisher's note

All claims expressed in this article are solely those of the authors and do not necessarily represent those of their affiliated organizations, or those of the publisher, the editors and the reviewers. Any product that may be evaluated in this article, or claim that may be made by its manufacturer, is not guaranteed or endorsed by the publisher.

References

Abbas, A. K., Flori, R. E., and Alsaba, M. (2019). Stability analysis of highly deviated boreholes to minimize drilling risks and nonproductive time. *J. Energy Resour. Technol.* 141 (8), 082904. doi:10.1115/1.4042733

Abdel-Fattah, M. I., Sen, S., Abuzied, S. M., Abioui, M., Radwan, A. A., and Benssaou, M. (2022). Facies analysis and petrophysical investigation of the late miocene Abu madi sandstones gas reservoirs from offshore baltim east field (nile Delta, Egypt). *Mar. Pet. Geol.* 137, 105501. doi:10.1016/j.marpetgeo.2021.105501

Abdel-Kireem, M. R., Schrank, E., Samir, A. M., and Ibrahim, M. I. A. (1996). Cretaceous palaeoecology, palaeogeography and palaeoclimatology of the northern Western Desert, Egypt. *J. Afr. Earth Sci.* 22 (1), 93–112. doi:10.1016/0899-5362(95)00125-5

Adly, O., El Araby, A. M., and El Barkooky, A. (2016). "Abu Roash F member as a potential self-sourced reservoir in Abu Gharadig Basin, Western Desert of Egypt," in *AAPG hedberg conference, the future of basin and petroleum systems modeling* (Santa Barbara, California). April 3–8. Search and Discovery Article #90257.

Ali, J., Ashraf, U., Anees, A., Peng, S., Umar, M. U., Thanh, H. V., et al. (2022). Hydrocarbon potential assessment of carbonate-bearing sediments in a meyal oil field, Pakistan: Insights from logging data using machine learning and quanti elan modeling. *ACS Omega* 7 (43), 39375–39395. doi:10.1021/acsomega.2c05759

Alyan, M., Martin, J., and Irwin, D. (2015). "Field development plan optimization for tight carbonate reservoirs," in *SPE Abu dhabi international petroleum exhibition and conference* (Abu Dhabi: UAE). Nov 9–12. SPE-177695-MS. doi:10.2118/177695-MS

Bashir, Y., Faisal, M. A., Biswas, A., Babasafari, A. A., Ali, S. H., Imran, Q. S., et al. (2021). Seismic expression of miocene carbonate platform and reservoir characterization through geophysical approach: Application in central luconia, offshore Malaysia. *J. Pet. Explor. Prod. Technol.* 11 (4), 1533–1544. doi:10.1007/s13202-021-01132-2

Bayoumi, A. I., and Lotfy, H. I. (1989). Modes of structural evolution of Abu Gharadig Basin, Western Desert of Egypt as deduced from seismic data. *J. Afr. Earth Sci.* 9 (2), 273–287. doi:10.1016/0899-5362(89)90070-5

Bosworth, W., El-Hawat, A. S., Helgeson, D. E., and Burke, K. (2008). Cyrenaican "shock absorber" and associated inversion strain shadow in the collision zone of northeast Africa. *Geology* 36 (9), 695–698. doi:10.1130/G24909A.1

Boutaleb, K., Baouche, R., Sadaoui, M., and Radwan, A. E. (2021). Sedimentological, petrophysical, and geochemical controls on deep marine unconventional tight limestone and dolostone reservoir: Insights from the Cenomanian/Turonian oceanic anoxic event 2 organic-rich sediments, Southeast Constantine Basin, Algeria. *Sediment. Geol.* 429, 106072. doi:10.1016/j.sedgeo.2021.106072

Chen, J. Q., Pang, X. Q., Wu, S., Chen, Z. H., Hu, M. L., Ma, K. Y., et al. (2020). Method for identifying effective carbonate source rocks: A case study from middle-upper ordovician in Tarim basin, China. *Pet. Sci.* 17 (6), 1491–1511. doi:10.1007/s12182-020-00489-z

Chimmalgi, V. S., Al-Humond, J., Al-Sabea, S., Gazi, N., Bardalaye, J., Mudavakkat, A., et al. (2013). "Reactivating a tight carbonate reservoir in the greater burgan field: Challenges, options and solutions," in *SPE Middle East oil and gas show and conference, Manama, Bahrain, March 10–13*. doi:10.2118/164248-MS

Curtis, J. B. (2002). Fractured shale-gas systems. *AAPG Bull* 86 (11), 1921–1938. doi:10.1306/61EEDDBE-173E-11D7-8645000102C1865D

Eaton, B. A. (1968). "Fracture gradient prediction and its application in oil field operations," in *SPE 43rd annual fall meeting*, Houston, Texas, September29–October 2, 25–32.

Egyptian General Petroleum Corporation (EGPC) (2019). *Production: Whole drilling report*.

El Atfy, H. (2011). *Cretaceous palynology of the GPTSW-7 well, Western Desert, Egypt*. Saarbrücken: LAP LAMBERT Academic Publishing.

El Beialy, S. Y., El Atfy, H. S., Zavada, M. S., El Khoriby, E. M., and Abu-Zied, R. H. (2010). Palynological, palynofacies, paleoenvironmental and organic geochemical studies on the Upper Cretaceous succession of the GPTSW-7 well, north Western Desert, Egypt. *Mar. Pet. Geol.* 27 (2), 370–385. doi:10.1016/j.marpetgeo.2009.10.006

El Diasty, W. (2014). Khatatba Formation as an active source rock for hydrocarbons in the northeast Abu Gharadig Basin, north Western Desert, Egypt. *Arab. J. Geosci.* 8 (4), 1903–1920. doi:10.1007/s12517-014-1334-x

El Gazzar, A. M., Moustafa, A. R., and Bentham, P. (2016). Structural evolution of the Abu Gharadig field area, northern Western Desert, Egypt. *J. Afr. Earth Sci.* 124, 340–354. doi:10.1016/j.jafrearsci.2016.09.027

El Shahat, W., Villinski, J. C., and El-Bakry, G. (2009). Hydrocarbon potentiality, burial history and thermal evolution for some source rocks in October oil field, northern Gulf of Suez, Egypt. *J. Pet. Sci. Eng.* 68 (3-4), 245–267. doi:10.1016/j.petrol.2009.06.018

El-Sherbiny, H. M. (2002). *Petrophysical evaluation of Abu el-gharadig basin, Egypt*. Ph.D. Dissertation, Cairo: Cairo University.

Farouk, S., Sen, S., Ganguli, S. S., Ahmad, F., Abioui, M., Al-Kahtany, K., et al. (2022). An integrated petrographical, petrophysical and organic geochemical characterization of the Lower Turonian Abu Roash-F carbonates, Abu Gharadig field, Egypt – inferences on self-sourced unconventional reservoir potential. *Mar. Pet. Geol.* 145, 105885. doi:10.1016/j.marpetgeo.2022.105885

Fea, I., Abioui, M., Nabawy, B. S., Jain, S., Bruno, D. Z., Kassem, A. A., et al. (2022). Reservoir quality discrimination of the albian-cenomanian reservoir sequences in the ivorian basin: A lithological and petrophysical study. *Geomech. Geophys. Geo-energ. Geo-resour.* 8 (1), 1. doi:10.1007/s40948-021-00297-8

Flügel, E. (2010). *Carbonate rocks. Analysis, interpretation and application*. 2nd edition. New York: Springer-Verlag, Berlin Heidelberg. doi:10.1007/978-3-642-03796-2

Ghassal, B. I., Littke, R., Atfy, H. E., Sindern, S., Scholtysik, G., El Beialy, S., et al. (2018). Source rock potential and depositional environment of Upper Cretaceous sedimentary rocks, Abu Gharadig Basin, Western Desert, Egypt: An integrated palynological, organic and inorganic geochemical study. *Int. J. Coal Geol.* 186, 14–40. doi:10.1016/j.coal.2017.11.018

Grieser, W. V., and Bray, J. M. (2007). "Identification of production potential in unconventional reservoirs," in *Production and operations symposium* (Oklahoma, USA: SPE). doi:10.2118/106623-MS

Guiraud, R., and Maurin, J. C. (1992). Early cretaceous rifts of western and central Africa: An overview. *Tectonophysics* 213 (1-2), 153–168. doi:10.1016/0040-1951(92)90256-6

Hajeri, S. A., Al Shehhi, A., Riberio, M. T., Ayoub, M., Negahban, S., and Bahmaish, J. (2007). "Tight reservoirs – a development challenge example from a carbonate reservoir, offshore Abu Dhabi, UAE," in *SPE Middle East oil & gas show and conference* (Manama: Kingdom of Bahrain). SPE-105420. doi:10.2118/105420-MS

Hakimi, M. H., Al-Matary, A. M., and Hersi, O. S. (2018). Late Jurassic bituminous shales from Marib oilfields in the Sabatayn Basin (NW Yemen): Geochemical and petrological analyses reveal oil-shale resource. *Fuel* 232, 530–542. doi:10.1016/j.fuel.2018.05.138

Hantar, G. (1990). "North Western Desert," in *The geology of Egypt*. Editor R. Said (Rotterdam, Brookfield: A.A. Balkema), 293–319.

Harishidayat, D., Farouk, S., Abioui, M., and Aziz, O. A. (2022). Subsurface fluid flow feature as hydrocarbon indicator in the Alamein Basin, onshore Egypt; Seismic attribute perspective. *Energies* 15 (9), 3048. doi:10.3390/en15093048

Herbin, J. P., Montadert, L., Muller, C., Gomez, R., Thurow, J., and Wiedmann, J. (1986). Organic-rich sedimentation at the cenomanian-turonian boundary in oceanic and coastal basins in the north atlantic and tethys. *Geol. Soc. Lond. Spec. Publ.* 21 (1), 389–422. doi:10.1144/GSL.SP.1986.021.01.28

Hewaidy, A. G., Elshahat, O. R., and Kamal, S. (2018). Stratigraphy, facies analysis and depositional environments of the upper unit of Abu Roash "E" member in the Abu Gharadig field, Western Desert, Egypt. *J. Afr. Earth Sci.* 139, 26–37. doi:10.1016/j.jafrearsci.2017.11.028

Hood, K. C., and Yurewicz, D. A. (2008). "Assessing the mesaverde basin-centered gas play, piceance basin, Colorado,". Editors S. P. Cumella, K. W. Shanley, and W. K. Camp. *Underst. Explor. Dev. tight-gas sands-2005 Vail Hedberg Conf.* (Tulsa: AAPG Hedberg Series), 3, 87–104. doi:10.1306/13131052H32776

Jarvie, D. M. (2012). "Shale resource systems for oil and gas: Part 1- shale-gas resource systems,". Editor J. A. Breyer. *Shale reservoirs-giant Resour. 21st century* (Tulsa: AAPG Memoir), 97, 69–87

Jiang, R., Zhao, L., Xu, A., Ashraf, U., Yin, J., Song, H., et al. (2022). Sweet spots prediction through fracture Genesis using multi-scale geological and geophysical data in the karst reservoirs of Cambrian Longwangmiao Carbonate Formation, Moxi-Gaoshiti area in Sichuan Basin, South China. *J. Pet. Explor. Prod. Technol.* 12 (5), 1313–1328. doi:10.1007/s13202-021-01390-0

Kassem, A. A., Hussein, W. S., Radwan, A. E., Anani, N., Abioui, M., Jain, S., et al. (2021a). Petrographic and diagenetic study of siliciclastic jurassic sediments from the northeastern margin of Africa: Implication for reservoir quality. *J. Pet. Sci. Eng.* 200, 108340. doi:10.1016/j.petrol.2020.108340

Kassem, A. A., Radwan, A. E., Santosh, M., Hussein, W. S., Abdelghany, W. K., Fea, I., et al. (2022). Sedimentological and diagenetic study of mixed siliciclastic/carbonate sediments in the propagation stage of Gulf of Suez rift basin, northeastern Africa: Controls on reservoir architecture and reservoir quality. *Geomech. Geophys. Geo-energ. Geo-resour.* 8 (6), 187. doi:10.1007/s40948-022-00502-2

Kassem, A. A., Sen, S., Radwan, A. E., Kassem, W. A., and Abioui, M. (2021b). Effect of depletion and fluid injection in the mesozoic and paleozoic sandstone reservoirs of the october oil field, central Gulf of Suez basin: Implications on drilling, production and reservoir stability. *Nat. Resour. Res.* 30 (3), 2587–2606. doi:10.1007/s11053-021-09830-8

Kenomore, M., Hassan, M., Dhakal, H., and Shah, A. (2017). Total organic carbon evaluation of the bowland shale formation in the upper bowland of the widmerpool Gulf. *J. Pet. Sci. Eng.* 150, 137–145. doi:10.1016/j.petrol.2016.11.040

Khalil Khan, H., Ehsan, M., Ali, A., Amer, M. A., Aziz, H., Khan, A., et al. (2022). Source rock geochemical assessment and estimation of TOC using well logs and geochemical data of Talhar Shale, Southern Indus Basin, Pakistan. *Front. Earth Sci.* 10, 969936. doi:10.3389/feart.2022.969936

Klemme, H. D., and Ulmishek, G. F. (1991). Effective petroleum source rocks of the world: Stratigraphic distribution and controlling depositional factors. *AAPG Bull* 75 (12), 1809–1851. doi:10.1306/0C9B2A47-1710-11D7-8645000102C1865D

Kumar, S., Ojha, K., Bastia, R., Gard, K., Das, S., and Mohanty, D. (2017). Evaluation of Eocene source rock for potential shale oil and gas generation in north Cambay Basin, India. *Mar. Pet. Geol.* 88, 141–154. doi:10.1016/j.marpetgeo.2017.08.015

Lang, J., Li, S., and Zhang, J. (2011). "Wellbore stability modeling and real-time surveillance for deep water drilling to weak bedding planes and depleted reservoirs," in *SPE/IADC drilling conference and exhibition held in amsterdam, The Netherlands, March 1–3. SPE-139708-MS*. doi:10.2118/139708-MS

Latief, A. I., Syofyan, S., Ab Hamid, T. M. T., Al Amoudi, M. A., and Shabibi, T. A. (2019). "Unlocking tight carbonate reservoir potential: Geological characterization

to execution," in *SPE Middle East oil and gas show and conference* (Bahrain: Manama). doi:10.2118/194712-MS

Leila, M., Sen, S., Abioui, M., and Moscariello, A. (2021). Investigation of pore pressure, *in-situ* stress state and borehole stability in the West and South Al-Khilala hydrocarbon fields, Nile Delta, Egypt. *Geomech. Geophys. Geo-energ. Geo-resour.* 7 (3), 56. doi:10.1007/s40948-021-00256-3

Lin, X. Y., and Su, X. B. (2007). Reservoiring mechanism of coalbed methane in southern Qinshui Basin. *Nat. Gas. Ind.* 27, 8–11.

Lin, X., Zeng, J., Wang, J., and Huang, M. (2020). Natural gas reservoir characteristics and non-Darcy flow in low-permeability sandstone reservoir of Sulige Gas Field, Ordos Basin. *Energies* 13 (7), 1774. doi:10.3390/en13071774

Lüning, S., Kolonic, S., Belhadj, E. M., Belhadj, Z., Cota, L., Baric, G., et al. (2004). Integrated depositional model for the Cenomanian-Turonian organic-rich strata in North Africa. *Earth-Sci. Rev.* 64 (1-2), 51–117. doi:10.1016/S0012-8252(03)00039-4

Makky, A. F., El Sayed, M. I., El-Ata, A. S. A., Abd El-Gaied, I. M., Abdel-Fattah, M. I., and Abd-Allah, Z. M. (2014). Source rock evaluation of some upper and lower Cretaceous sequences, West Beni Suef concession, Western Desert, Egypt. *Egypt. J. Pet.* 23 (1), 135–149. doi:10.1016/j.ejpe.2014.02.016

Militzer, H., and Stoll, R. (1973). Einige Beiträge der Geophysik zur primärdatenerfassung im Bergbau. *Neue Bergbautech.* 3, 21–25.

Moretti, I., Kerdraon, Y., Rodrigo, G., Huerta, F., Griso, J. J., Sami, M., et al. (2010). South alamein petroleum system (Western Desert, Egypt). *Pet. Geosci.* 16 (2), 121–132. doi:10.1144/1354-079309-004

Ozkan, A., Milliken, K. L., Macaulay, C., Johnston, M., Minisini, D., Eldrett, J. S., et al. (2013). "Influence of primary rock texture, diagenesis, and thermal maturity on Eagle Ford pore systems," in Annual Convention and Exhibition, Pittsburgh, Pennsylvania, USA, May 19–22 . AAPG Search and DiscoveryArticle #90163.

Peters, K. E. (1986). Guidelines for evaluating petroleum source rock using programmed pyrolysis. *AAPG Bull.* 70 (3), 318–329. doi:10.1306/94885688-1704-11D7-8645000102C1865D

Plumb, R. A., Evans, K. F., and Engelder, T. (1991). Geophysical log responses and their correlation with bed to bed stress contrasts in Paleozoic rocks, Appalachian Plateau, New York. *J. Geophys. Res.* 96 (9), 14509–14528. doi:10.1029/91JB00896

Radwan, A. E., Trippetta, F., Kassem, A. A., and Kania, M. (2021). Multi-scale characterization of unconventional tight carbonate reservoir: Insights from October oil filed, Gulf of Suez rift basin, Egypt. *J. Pet. Sci. Eng.* 197, 107968. doi:10.1016/j.petrol.2020.107968

Salah, M., Orr, D., Meguid, A. A., Crane, B., and Squires, S. (2016). "Multistage horizontal; fracture optimization through an integrated design and workflow in Apollonia Tight Chalk, Egypt from the laboratory to the field," in *Abu dhabi international petroleum exhibition & conference, Abu dhabi, UAE, nov 7–10*. SPE-183068. doi:10.2118/183068-MS

Salama, A. M., Abd-Allah, Z. M., El-Sayed, M. I., and Elbastawesy, M. A. (2021). Source rock evaluation and burial history modeling of cretaceous rocks at the khalda concession of Abu Gharadig Basin, Western Desert, Egypt. *J. Afr. Earth Sci.* 184, 104372. doi:10.1016/j.jafrearsci.2021.104372

Salamy, S. P., Al-Mubarak, H. K., Al-Ghamdi, M. S., and Hembling, D. E. (2008). Maximum-reservoir-contact-wells performance update: Shaybah field, Saudi arabia. *SPE Prod. Oper.* 23 (4), 439–443. doi:10.2118/105141-PA

Saleri, N. G., Salamy, S. P., Mubarak, H. K., Sadler, R. K., Dossary, A. S., and Muraikhi, A. J. (2004). Shaybah-220: A maximum-reservoir-contact (MRC) well and its implications for developing tight-facies reservoirs. *SPE Res. Eval. Eng.* 7 (04), 316–320. doi:10.2118/88986-PA

Sarhan, M. A., and Basal, A. M. K. (2020). Total organic carbon content deduced from resistivity-porosity logs overlay: A case study of Abu Roash formation, southwest qarun field, gindi basin, Egypt. *NRIAG J. Astron. Geophys.* 9 (1), 190–205. doi:10.1080/20909977.2020.1736761

Sarhan, M. A., and Collier, R. E. L. (2018). Distinguishing rift-Related from inversion-related anticlines: Observations from the Abu Gharadig and gindi basins, Western Desert, Egypt. *J. Afr. Earth Sci.* 145, 234–245. doi:10.1016/j.jafrearsci.2018.06.004

Sarhan, M. A. (2017). Wrench tectonics of Abu Gharadig Basin, Western Desert, Egypt: A structural analysis for hydrocarbon prospects. *Arab. J. Geosci.* 10 (18), 399. doi:10.1007/s12517-017-3176-9

Sen, S., Abioui, M., Ganguli, S. S., Elsheikh, A., Debnath, A., Benssaou, M., et al. (2021). Petrophysical heterogeneity of the early Cretaceous Alamein dolomite reservoir from North Razzak oil field, Egypt integrating well logs, core measurements, and machine learning approach. *Fuel* 306, 121698. doi:10.1016/j.fuel.2021.121698

Shalaby, A., and Sarhan, M. A. (2021). Origin of two different deformation styles via active folding mechanisms of inverted Abu El Gharadiq Basin, Western Desert, Egypt. *J. Afr. Earth Sci.* 183, 104331. doi:10.1016/j.jafrearsci.2021.104331

Strating, E. H. H., and Franssen, R. C. M. W. (2006). "Discovering and developing a deep jurassic play in the mature Western Desert, Abu Gharadig Basin, Egypt," in SPE europec/EAGE annual conference and exhibition, Vienna, Austria, June 12-15. SPE-100125. doi:10.2118/100125-MS

Taghipour, M., Ghafoori, M., Lashkaripour, G. R., Hafezi Moghaddas, N., and Molaghab, A. (2019). Estimation of the current stress field and fault reactivation analysis in the Asmari reservoir, SW Iran. *Pet. Sci.* 16 (3), 513–526. doi:10.1007/s12182-019-0331-9

Ullah, S., Jan, I. U., Hanif, M., Latif, K., Mohibullah, M., Sabba, M., et al. (2022). Paleoenvironmental and bio-sequence stratigraphic analysis of the cretaceous pelagic carbonates of eastern tethys, sulaiman range, Pakistan. *Minerals* 12 (8), 946. doi:10.3390/min12080946

Wei, Li, Tu, J., Zhang, J., and Zhang, B. (2017). Accumulation and potential analysis of self-sourced natural gas in the ordovician majiagou Formation of Ordos basin, NW China. *Pet. Explor. Dev.* 44 (4), 552–562. doi:10.1016/S1876-3804(17)30064-2

Yang, X. (2020). Characteristics of mesozoic hydrocarbon source rocks and distribution of remaining resources in the Western Desert Basin of Egypt. *Oil Gas. Geol.* 41 (2), 423–433.

Zhang, J. (2013). Borehole stability analysis accounting for anisotropies in drilling to weak bedding planes. *Int. J. Rock Mech. Min. Sci.* 60, 160–170. doi:10.1016/j.ijrmms.2012.12.025

Zhang, W., Gao, J., Lan, K., Liu, X., Feng, G., and Ma, Q. (2015). Analysis of borehole collapse and fracture initiation positions and drilling trajectory optimization. *J. Pet. Sci. Eng.* 129, 29–39. doi:10.1016/j.petrol.2014.08.021

Zhao, J. L., Gong, Z. W., Li, E., Feng, C. Y., Bai, X., and Jian, J. (2012). A review and perspective of identifying and evaluating the logging technology of fractured carbinate reservoir. *Prog. Geophys.* 27 (2), 537–547

Zobaa, M. K., Oboh-Ikuenobe, F. E., Ibrahim, M. I., Arneson, K. K., Browne, C. M., and Kholeif, S. (2009).The cenomanian/turonian oceanic anoxic event in the razzak #7 oil well, north Western Desert, Egypt: Palynofacies and isotope analyses. *GSA annual meeting, abstracts with programs*. Portland, Oregon: USA, 513

Zobaa, M. K., Oboh-Ikuenobe, F. E., and Ibrahim, M. I. (2011). The cenomanian/turonian oceanic anoxic event in the razzak field, north Western Desert, Egypt: Source rock potential and paleoenvironmental association. *Mar. Pet. Geol.* 28 (8), 1475–1482. doi:10.1016/j.marpetgeo.2011.05.005

Zoback, M. D., and Lund Snee, J. E. (2018). "Predicted and observed shear on preexisting faults during hydraulic fracture stimulation," in *SEG technical program expanded abstracts* (Tulsa: Society of Exploration Geophysicists), 3588–3592. doi:10.1190/segam2018-2991018.1